FULL POLARIMETRIC TIME SERIES IMAGE ANALYSIS FOR CROP TYPE MAPPING

H. Noroozi [1], M. Hasanlou [1]

[1] School of Surveying and Geospatial Engineering, College of Engineering, University of Tehran, Tehran, Iran

(helia.noroozi, hasanlou@ut.ac.ir)

Commission IV, WG IV/3

KEY WORDS: Crop type, RADARSAT 2, Polarimetry, Machine learning, Random Forest, Cat Boost

ABSTRACT:

Crop information and quality are not only fundamental for experts using spatial decision support systems but also have many applications in irrigation management, economic analysis for import or export, food safety, and achieving sustainable agriculture. Remote sensing is a cheap and fast way of reaching this goal. Full polarimetric SAR unlike optical sensors is an all-weather system providing geometrical and physical properties of the earth's surface events. Due to the dynamic changes in crop properties through their phenological stages, crop type mapping has been challenging. As a result, accurate, reliable, and cost-effective crop type mapping using minimum data and processing has been the goal of the remote sensing and precision agriculture community. In this study, a new method based on time series analysis of full polarimetric SAR data combined with radar indices, polarimetric decompositions followed by the three αs extracted from H/A/α decomposition, and unsupervised H/α/Wishart classification bands as features generated from only 5 dates of RADARSAT CONSTELLATION MISSION 2 data were used for classification of crops. Applying random forest and cat boost algorithm as classifiers an accuracy of 87.4% and 75% was respectively achieved. indicating that both algorithms have promising results. Although the random forest algorithm had better results, the cat boost algorithm had less noise in each field and more homogenous farms were detected.

1. INTRODUCTION

Due to the rapidly growing acreage of crops, the abruptly increasing population of the world, new global legislations, and the necessity of minimizing the environmental footprint precision agriculturally based actions through remote sensing must be taken to overcome these problems (Jafarbiglu and Pourreza, 2022). One of these actions is crop-type mapping using Optical, SAR, or a fusion of both data sources. Optical data e.g., LIDAR or hyperspectral images impose high acquisition and computational costs (Moradi et al, 2021). Whereas, SAR observations compared to optical sensors are all-weather mapping systems which is the main advantage of SAR images (Yekkehkhany et al, 2014). Making it suitable for Nordic, humid, and mostly cloudy countries e.g., Canada and Greenland. Synthetic aperture radar (SAR) in its different acquisition modes, provides different features regarding the object's physical, geometrical, and structural properties. As a result, it is useful in Remote Sensing and Photogrammetric research including crop type mapping (Adrian et al., 2021; Saadat et al, 2019; Tufail et al, 2022), change detection (Habibollahi, 2022; Saha, 2020), flood monitoring (Carreño Conde and De Mata Muñoz, 2019), Earthquake damage monitoring (Hasanlou, 2021), precision agriculture, oceanography (Zheng, 2019), etc. based on the number of acquired channels SAR images are classified as single, dual, and quad (full) polarizations which contain all the VV and HH known as co-polarizations and VH and HV known as cross-polarizations. As the number of channels rises, so will the number of features and resulting properties, therefore increasing the accuracy. Due to the difference in dielectric properties and the structure of the different crop types, a distinct variation is seen for

This contribution has been peer-reviewed. The double-blind peer-review was conducted on the basis of the full paper.
https://doi.org/10.5194/isprs-annals-X-4-W1-2022-603-2023 | © Author(s) 2023. CC BY 4.0 License.

properties such as the size, shape, and orientation distribution of the scatterers (crops) through the growing season due to the development of crops making it possible to classify different crops in SAR images (Skriver et al, 1999; Yekkehkhany et al, 2014). Therefore, requiring multi-temporal image acquisition and time series analysis in important or all phenological stages of different crops. One of the important products derived from the Full Polarimetric SAR observations is called the scattering matrix (T3) which contains a very important source of information about the terrestrial targets (Van Zyl et al, 1990). Thus, used in many physical studies. on the other hand, using the co and cross-polarized bands different indices can be generated through mathematical operations such as Radar Vegetation Index (RVI) (Kim et al, 2011), Radar Forest Degradation Index (RFDI) (Mitchard et al, 2012), Canopy Structure Index (CSI) (Sims and Gamon, 2003), co and cross ratios i.e., HH/VV, VV/VH, and HH/HV, etc. In addition to the mentioned methods for increasing the number of features, it is possible to use different decompositions such as H/ A/ α proposed by Cloude and Pottier (Cloude and Pottier, 1997), Pauli, Freeman- Durden (Freeman and Durden, 1993), and Cloude. Adding these features to the scattering matrix increases the possibility of more accurate classification of complex features like crops.

Crop type mapping using SAR images has been assessed in different studies (Yekkehkhany et al, 2014) used JPL-NASA UAVSAR data and SVM with RBF kernel as the classifier, archiving an overall accuracy (OA) of 85.52%. (Mahdianpari et al, 2019) achieved an OA of 84.30% on RADARSAT Constellation Mission (RCM) data on full polarimetric images using a random forest classifier. (Busquier et al, 2019) used TANDEMX data with coherency bands for co and cross-polarized bands at 6 dates achieving an OA of 89.01%, (Gella et al, 2021) used twDTW on long-term Terra SARX data achieving an OA of 80.6%. In this research, we proposed a method based on different indices, and decompositions and added an unsupervised classified map as a new channel to generate reliable features for accurate crop type mapping using only 5 dates of RCM data. Classification is conducted using Random Forest and Cat Boost algorithms. Random Forest is implemented in two stages: 1. learners' creation, and 2. outputs combination (Moradi et al, 2021) and has been used in many agricultural studies e.g., (Sedaghat et al, 2022) used it for surface soil moisture estimation, (Shahrayini and Noroozi 2021) used it for soil salinity and alkalinity mapping and (Shahrayini et al, 2022) used it for multi-depth soil carbon modeling. Cat Boost is an algorithm for gradient boosting on decision trees that were the winner of the Kenya crop type mapping challenge in 2020. Moreover, it has been used in the estimation of aboveground biomass (Luo et al, 2021; Zhang et al, 2020) and fire prediction (Zhou et al, 2021) but not for crop type mapping using polarimetric data. Evaluation is carried out in terms of overall accuracy and kappa coefficient. The classification was done in python using Sklearn, Numpy, Rasterio, and cv2 libraries in python 3.8.8.

2. MATERIALS AND METHOD

RADARSAT 2 is a C-band Canadian Space Agency Earth observation satellite launched on 14 December 2007. It acquires data in full polarimetric mode and different spatial resolutions for different products. The data used in this paper is for Carman, Manitoba, Canada in 2020 from RADARSAT 2 in 5 dates as shown in Table 1. All images are in simple look complex (SLC) mode with 9 meters ground resolution and 20-kilometer swath width.

Table 1. Data acquisition time.

2020/07/23	2020/08/24
2020/08/16	2020/09/09
2020/09/17	

To classify crops using the proposed supervised method ground truth (GT) data is required, which was acquired from Google Earth Engine's (GEE) AAFC product generated from Sentinel-1, 2, and Landsat missions with 30meter spatial resolution in 2020. However, due to the difference in the resolution of GT and RCM data, resampling was conducted using the bilinear resampling method.

The proposed framework in this paper consists of four main steps: (a) data preprocessing, (b) processing, (c) classification, and (d) evaluation. Several polarimetric features are extracted from preprocessed data i.e., the coherency or covariance matrix (T3). Span (total backscattered power), decompositions including H/A/α, Freeman-Durden, Paulie, and Cloude followed by radar indices including RVI, RFDI, CSI, Biomass index (BMI) also known as average like-polarized and Volume Scattering index (VSI) the is mostly caused by a canopy and defined using average cross-polarized and BMI (Pope et al. 1994). All these bands are extracted and used as features for each time step resulting in 26 features for each time step and 130 total features. Finally, random forest (RF) and cat boost classification algorithms were applied. Their results were compared to find the best model for the classification of different crops using the generated features and RCM time series images. The complete method is shown in Figure 1.

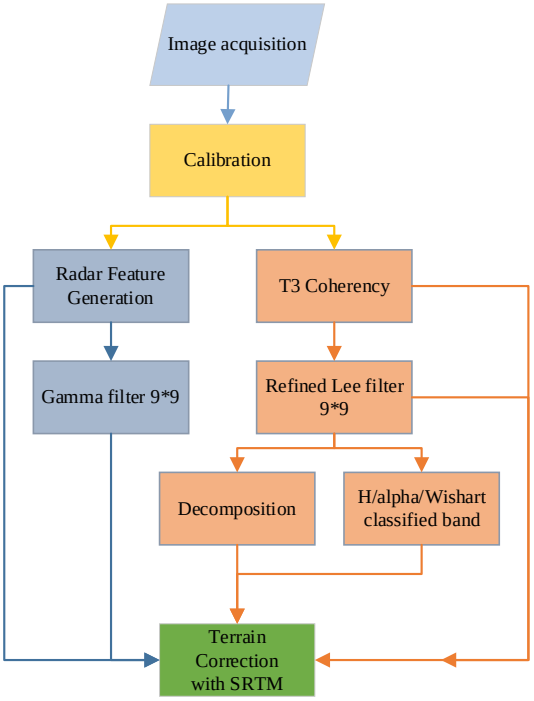

Figure 1. Flowchart of the proposed method.

Preprocessing includes 1. Calibration, and 2. Applying a Radar speckle filter to reduce noise using a Gamma filter with 9×9 kernel on radar indices. Processing steps include 1. Polarimetric coherency matrix generation, speckle filter to reduce noise using Refined Lee filter 9×9 on T3 matrix, decompositions, and features generation, 2. Geometric correction using range doppler train correction method and SRTM DEM (30m). the complete pre-processing and processing were repeated for each time step in SNAP software. The formulas for generated indices and Span are shown in Table 2.

Table 2. Formulas for generated indices and Span

Index	Formula
RVI	$\frac{8\sigma_{hv}}{\sigma_{vv} + \sigma_{hh} + 2\sigma_{hv}}$
RFDI	$\frac{\sigma_{hh} - \sigma_{hv}}{\sigma_{hh} + \sigma_{hv}}$
CSI	$\frac{VV}{VV + HH}$
CS	$\frac{HV + VH}{2}$
LK	$\frac{VV + HH}{2}$
VSI	$\frac{CS}{CS + LK}$
BMI	LK
Span	HH + 2HV + VV

where σ_{hh} is the corrected radar backscatter coefficient.

Some of these features are shown in Figures 2 and 3.

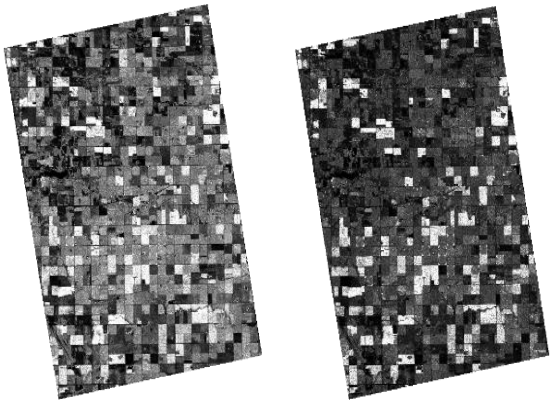

Figure 2. Span and RVI

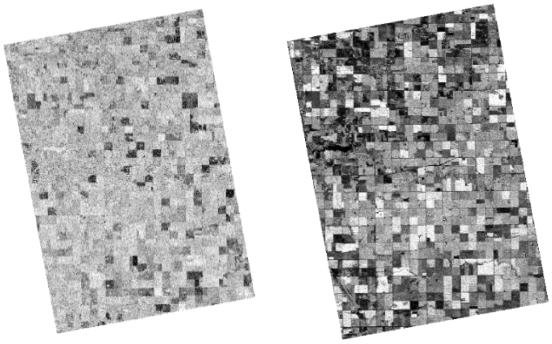

Figure 3. CSI and BMI

The generated decompositions and the H/ α /Wishart classified bands are shown in Figures 4, 5, and 6.

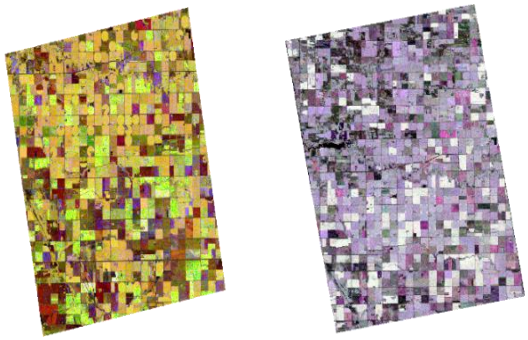

Figure 4. Freeman- Durden and Paulie decompositions

This contribution has been peer-reviewed. The double-blind peer-review was conducted on the basis of the full paper.
https://doi.org/10.5194/isprs-annals-X-4-W1-2022-603-2023 | © Author(s) 2023. CC BY 4.0 License.

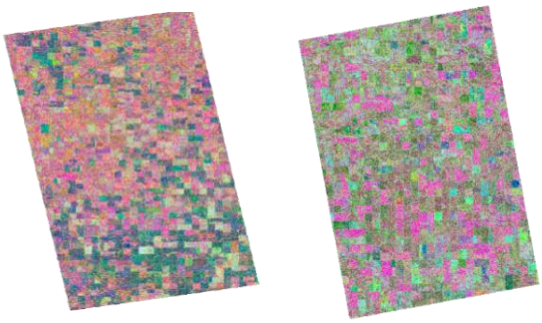

Figure 5. H/A/α and Cloude decompositions

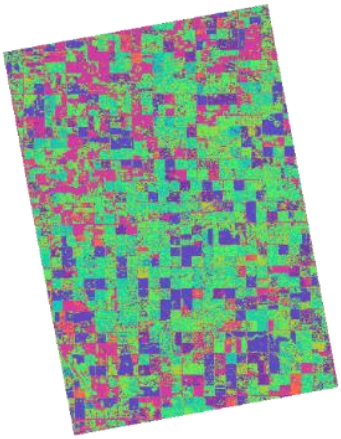

Figure 6. H/ α /Wishart classified band

Since some of these images have different footprints and processing these images is time-consuming, all bands were clipped to a smaller area of 1395×765 pixels with 12 classes of crops and other land cover classes in Arc Map 10.7. furthermore, all bands were projected to UTM Zone 14N so all bands are in the same coordinate system. The ground truth and its corresponding legend, are shown in Figure 7.

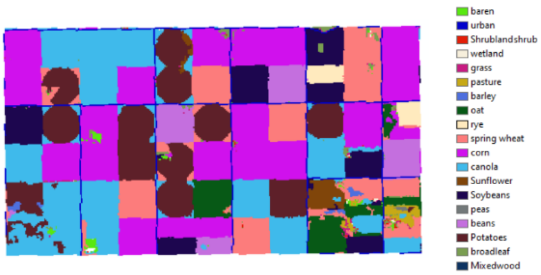

Figure 7. Ground truth with Legend

Finally, 60% of these images were divided to train for training the classifiers and the remaining 40% were considered as test data for evaluating the algorithm. To train RF efficiently these settings were applied: 300 trees, 100 maximum features, and a minimum sample split of 2 at each node. As for the cat boost classification algorithm learning rate of 0.1, random strength of 0.1, depth of 12, and a multi-class loss function with 150 iterations were considered.

3. RESULTS

The proposed method is applied to the extracted multi-temporal polarimetric bands. Based on the GT (shown in Figure 5), several types of crop classes are considered including Soybeans, Sunflower, Wheat, Canola, Corn, Rye, Oats, Beans, Broadleaf, Potato, and Peas. Also, classes of mixed wood, barren land, and shrub land were included in the ground truth. Classified maps using RF and cat boost are shown in Figure 8.

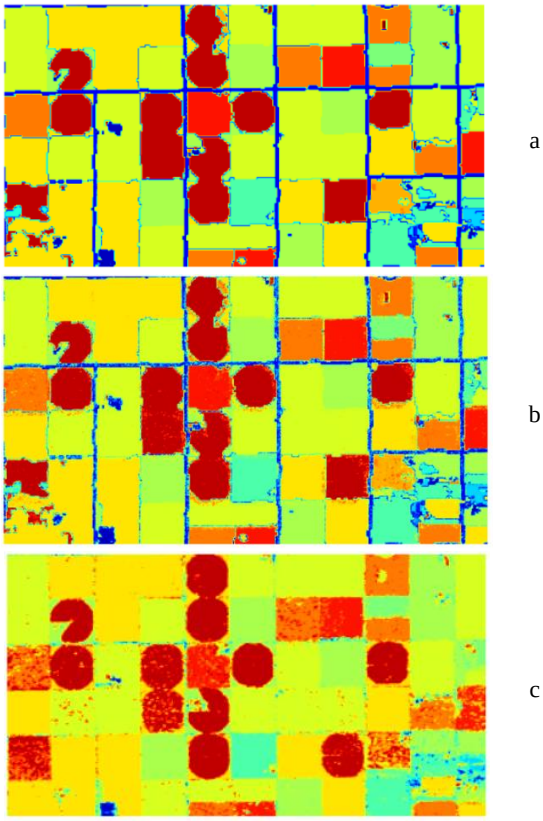

Figure 8. (a) Ground truth, (b) RF predicted map, (c) Cat Boost predicted map.

Validation was carried out using the accuracy metrics of OA and Kappa which are illustrated in Table 3.

Table 3. Accuracy Metrics

Algorithm	OA (%)	Kappa
RF	87.4	0.849
Cat Boost	74.9	0.698

4. CONCLUSION

As shown in Table 3, through the proposed method and the mentioned features we were able to achieve reasonable accuracy on only 5 dates of images for RCM data in discriminating different crops and earth surface features. It can be seen that RF had higher accuracy. Although both algorithms are pixel-based and trained on vectorized data, the map generated from RF has more noise in each field compared to the map resulting from the Cat Boost algorithm which classified each farm homogenously, in other words, it functioned like an object-based classifier even though it is a pixel-based classifier. Both classifiers had promising results, low processing time, and functioned properly with a low amount of data making them time-efficient and reliable.

In this paper, the use of canopy-related radar features, span, and different decompositions derived from a series of RADARSAT2 SLC images in summer 2020 was assessed for crop type mapping. The reviewed papers either used a coarser, longer time series, images with higher spatial resolution e.g., TANDEMX spotlight mode with 1m resolution, or a combination of all the above-mentioned data and reached a maximum accuracy of less than 87%. On the other hand, studies on RADARSAT2 reached a maximum OA of 84.30% which is less than our proposed method which reached an OA of 87%. This method was trained on only 60% of the data and only five dates during the summer. Also, it is not only sensitive to the crop types but also sensitive to other land cover classes such as barren land, urban, mixed wood, shrubland, and field boundaries making it suitable for future purposes of agricultural cadaster, planning, and monitoring. RF is a fast, low memory-consuming classifier and can be trained on low data unlike recent deep learning approaches that are data hungry, slow and require station systems making them inefficient for Polarimetric studies because these datasets aren't easily or freely available, especially in higher resolutions, longer time series or larger scales with their relative ground truths. In conclusion, this method is accurate, fast, and reliable. Researchers are suggested to test other canopy-related features and test their impact on classification accuracy.

5. ACKNOWLEDGEMENTS

The authors would like to thank the NASA ARSET team for sharing Radarsat2 images out of charge to the public on their website.

REFERENCES

Adrian, J., V. Sagan, and M. Maimaitijiang, 2021: Sentinel SAR-optical fusion for crop type mapping using deep learning and Google Earth Engine. *ISPRS Journal of Photogrammetry and Remote Sensing*, 175, 215-235.

Busquier, M., J. M. Lopez-Sanchez, and D. Bargiel, 2019: Added value of coherent copolar polarimetry at X-band for crop-type mapping. *IEEE Geoscience and Remote Sensing Letters*, 17, 819-823.

Carreño Conde, F., and M. De Mata Muñoz, 2019: Flood monitoring based on the study of Sentinel-1 SAR images: The Ebro River case study. *Water*, 11, 2454.

Cloude, S. R., and E. Pottier, 1997: An entropy based classification scheme for land applications of polarimetric SAR. *IEEE transactions on geoscience and remote sensing*, 35, 68-78.

Freeman, A., and S. L. Durden, 1993: Three-component scattering model to describe polarimetric SAR data. *Radar Polarimetry*, SPIE, 213-224.

Gella, G. W., W. Bijker, and M. Belgiu, 2021: Mapping crop types in complex farming areas using SAR imagery with dynamic time warping. *ISPRS journal of photogrammetry and remote sensing*, 175, 171-183.

Habibollahi, R., S. T. Seydi, M. Hasanlou, and M. Mahdianpari, 2022: TCD-Net: A novel deep learning framework for fully polarimetric change detection using transfer learning. *Remote Sensing*, 14, 438.

Hasanlou, M., R. Shah-Hosseini, S. T. Seydi, S. Karimzadeh, and M. Matsuoka, 2021: Earthquake damage region detection by multitemporal coherence map analysis of radar and multispectral imagery. *Remote Sensing*, 13, 1195.

Jafarbiglu, H., and A. Pourreza, 2022: A comprehensive review of remote sensing platforms, sensors, and applications in nut crops. *Computers and Electronics in Agriculture*, 197, 106844.

Kim, Y., T. Jackson, R. Bindlish, H. Lee, and S. Hong, 2011: Radar vegetation index for estimating the vegetation water content of rice and soybean. *IEEE Geoscience and Remote Sensing Letters*, 9, 564-568.

Luo, M., Y. Wang, Y. Xie, L. Zhou, J. Qiao, S. Qiu, and Y. Sun, 2021: Combination of feature selection and catboost for prediction: The first application to the estimation of aboveground biomass. *Forests*, 12, 216.

Mahdianpari, M., F. Mohammadimanesh, H. McNairn, A. Davidson, M. Rezaee, B. Salehi, and S. Homayouni, 2019: Mid-season crop classification using dual-, compact-, and full-polarization in preparation for the Radarsat Constellation Mission (RCM). *Remote Sensing*, 11, 1582.

Mitchard, E. T., and Coauthors, 2012: Mapping tropical forest biomass with radar and spaceborne LiDAR in Lopé National Park, Gabon: overcoming problems of high biomass and persistent cloud. *Biogeosciences*, 9, 179-191.

Moradi, F., F. D. Javan, and A. Toosi, 2021: Tree detection using UAV based imagery system based on Random Forest classification.

Pope, K. O., J. M. Rey-Benayas, and J. F. Paris, 1994: Radar remote sensing of forest and wetland ecosystems in the Central American tropics. *Remote Sensing of Environment*, 48, 205-219.

Saadat, M., M. Hasanlou, and S. Homayouni, 2019: RICE CROP MAPPING USING SENTINEL-1 TIME SERIES IMAGES (CASE STUDY: MAZANDARAN, IRAN). *International Archives of the Photogrammetry, Remote Sensing & Spatial Information Sciences*.

Saha, S., F. Bovolo, and L. Bruzzone, 2020: Building change detection in VHR SAR images via unsupervised deep transcoding. *IEEE Transactions on Geoscience and Remote Sensing*, 59, 1917-1929.

Sedaghat, A., M. S. Shahrestani, A. A. Noroozi, A. F. Nosratabad, and H. Bayat, 2022: Developing pedotransfer functions using Sentinel-2 satellite spectral indices and Machine learning for estimating the surface soil moisture. *Journal of Hydrology*, 606, 127423.

Shahrayini, E., and A. A. Noroozi, 2021: Modeling And Mapping of Soil Salinity And Alkalinity Using Remote Sensing Data And Topographic Factors.

Shahrayini, E., H. Shafizadeh-Moghadam, A. A. Noroozi, and M. K. Eghbal, 2022: Multiple-depth modeling of soil organic carbon using visible–near infrared spectroscopy. *Geocarto International*, 37, 1393-1407.

Sims, D. A., and J. A. Gamon, 2003: Estimation of vegetation water content and photosynthetic tissue area from spectral reflectance: a comparison of indices based on liquid water and chlorophyll absorption features. *Remote sensing of environment*, 84, 526-537.

Skriver, H., M. T. Svendsen, and A. G. Thomsen, 1999: Multitemporal C-and L-band polarimetric signatures of crops. *IEEE Transactions on Geoscience and Remote Sensing*, 37, 2413-2429.

Tufail, R., A. Ahmad, M. A. Javed, and S. R. Ahmad, 2022: A machine learning approach for accurate crop type mapping using combined SAR and optical time series data. *Advances in Space Research*, 69, 331-346.

Van Zyl, J., 1990: Scattering matrix representations for simple targets. *Radar polarimetry for geoscience applications*.

Yekkehkhany, B., A. Safari, S. Homayouni, and M. Hasanlou, 2014: A comparison study of different kernel functions for SVM-based classification of multi-temporal polarimetry SAR data. *The International Archives of Photogrammetry, Remote Sensing and Spatial Information Sciences*, 40, 281.

Zhang, Y., J. Ma, S. Liang, X. Li, and M. Li, 2020: An evaluation of eight machine learning regression algorithms for forest aboveground biomass estimation from multiple satellite data products. *Remote Sensing*, 12, 4015.

Zheng, G., X. Li, and B. Liu, 2019: AI-Based Remote Sensing Oceanography-Image Classification, Data Fusion, Algorithm Development and Phenomenon Forecast. *IGARSS 2019-2019 IEEE International Geoscience and Remote Sensing Symposium*, IEEE, 7940-7943.

Zhou, F., H. Pan, Z. Gao, X. Huang, G. Qian, Y. Zhu, and F. Xiao, 2021: Fire Prediction Based on CatBoost Algorithm. *Mathematical Problems in Engineering*, 2021.